# A new sensor for detecting and characterising acoustic cavitation in vivo during ESWL

F Fedele, A J Coleman, T G Leighton, P R White and A M Hurrell

Extracorporeal Shock-Wave Lithotripsy (ESWL) is the leading technique for the non-invasive treatment of kidney, ureteric and biliary stones. It was first **(1)** introduced in 1981 to treat kidney stones. Nowadays it is also being used in the cure of salivary stones and management of some orthopaedic diseases **(2-4)**.

Lying on a table, the patient is coupled to an external ultrasound shock source through a water cushion *(Figure 1)*. Thousands of ultrasound shocks, with peak-positive pressure up to 100MPa, are focused on the stone in order to break it into fragments small enough to be passed naturally by the body. The stone is localised using x-ray and ultrasound (US) systems.

The shock source may belong to one of three different families **(5)**: electrohydraulic (EH), piezoelectric (PZ) and electromagnetic (EM). The two lithotripters used in this study have an EM source. The shock is generated by a high-voltage capacitor discharging through a flat coil coupled to a copper membrane, which is fixed at the end of a shock tube *(Figure 2)*. Though the procedure is well established, the re-treatment rate **(6)** is still around 50 per cent.

Both x-ray and US systems are affected by alignment errors **(7)**. Several projects have examined the development of auxiliary targeting techniques that may identify if the stone has actually been hit by the beam **(8-10)**. Olson *et al* **(10)** suggested a system based on the classification of the audible sound that is generated when the shock hits the stone, while other authors **(8-9)** worked on solutions based on the elaboration of ultrasound echoes from signals generated by active ultrasonic probes.

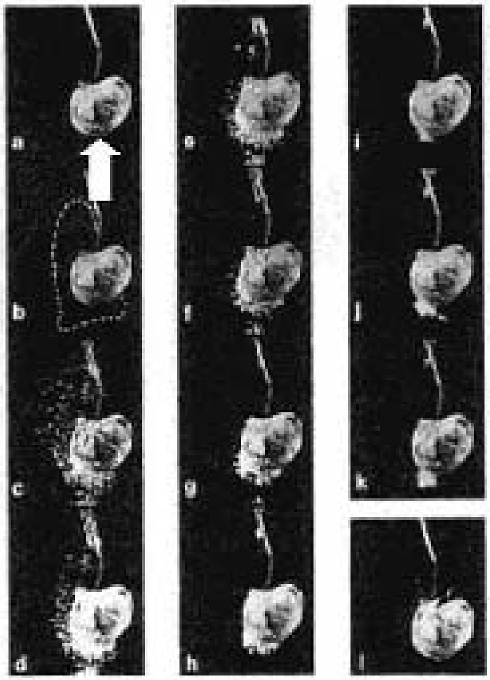


**Figure 3** Sequence of high speed photographic pictures of human gallstone being hit by a shock wave in Sass et al 1991. The interval between each frame is of 01ms *(a)* Taken 01ms prior to the shock hitting the stone. The white arrow indicates the shock orientation. The shock reaches the stones between (a) and *(b) (b-h)*. These frames show cavitation activity. Note bubbles on the stone referring to cavitation within small cracks *(i-k)*. Rapid material outburst *(l)* Disintegration of the stone within the crack

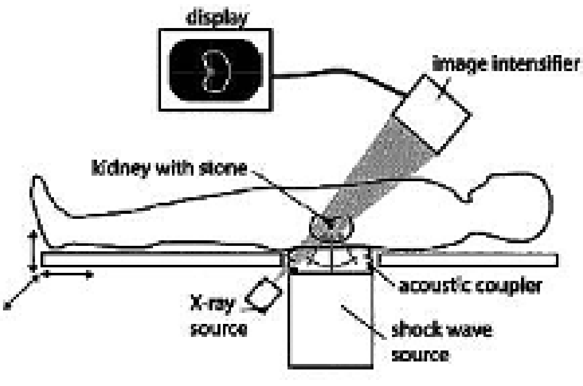


**Figure 1** Schematic of Lithotripsy

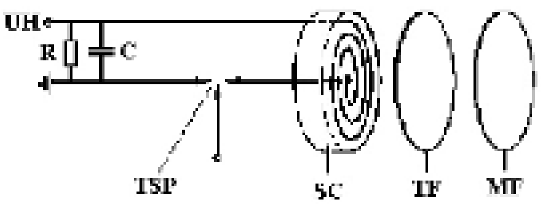


**Figure 2** Schematic representation of the EM source (TSP) Triggered spark-gap (SC) Flat solenoid (IF) Polyamide film (MF) Copper membrane

A significant limitation of the present lithotripters is that there is no capability for on-line monitoring of the degree of fragmentation of the stone. Usually the urologist tries to assess this by observing if any changes appear in the density or size of the stone in the x-ray image. Frequent checks may be done if low dose x-ray fluoroscopy is used, but a continuous monitoring can not be used to limit the patient's x-ray dose, and the method does not provide a quantitative measurement of the grade of fragmentation of the stone.

The underlying physical mechanisms responsible for fragmentation of the stone are still subject to investigation. Several studies indicate that both direct stress damage and indirect cavitation erosion seem to be necessary to obtain eliminable fragments **(11)**. The impacting shockwave produces the first fissures in the stone *(Figure 3)*. Later cavitation bubbles imploding within these splits cause the actual disintegration **(12)**.

In previous studies the authors **(13)** monitored cavitation *in-vivo* through the associated acoustic emissions, exploiting an experimental focused piezoelectric bowl. The objective of this study was to design a new passive and unfocused acoustic sensor to detect and characterise cavitation *in vivo* during ESWL.

The first phase of the study used an experimental cavitation sensor (*Figure 4*, developed by the National

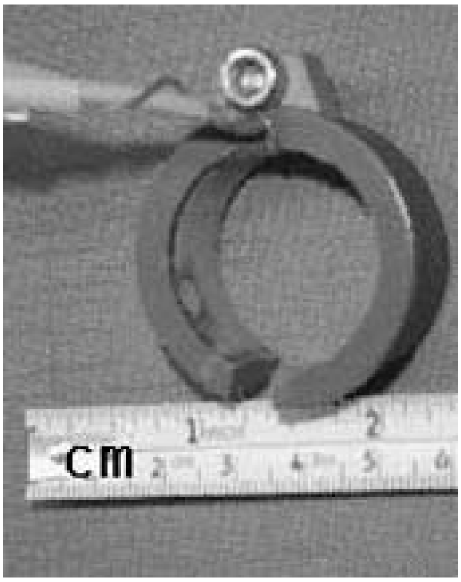


**Figure 4** NPL cylindrical cavitation sensor

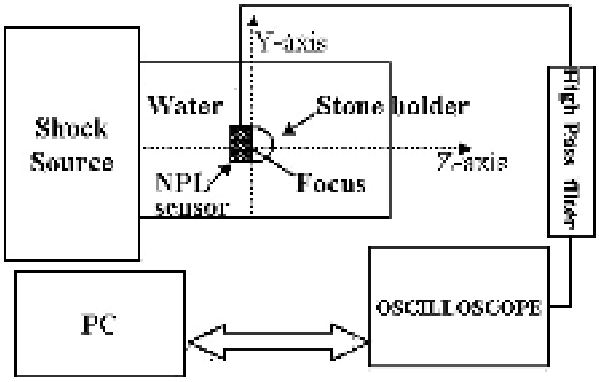


**Figure 6** Experimental set-up

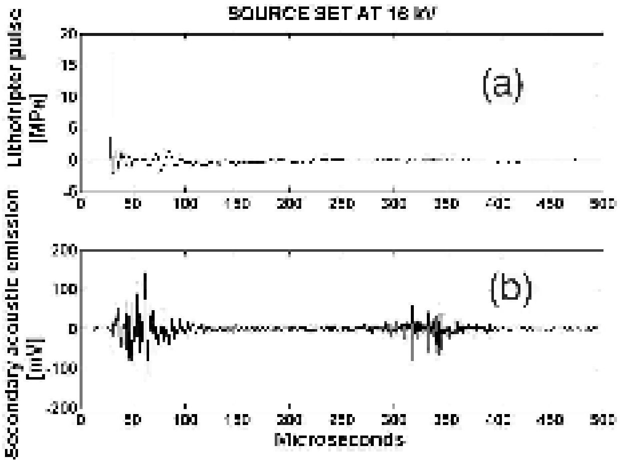


**Figure 7 (a)** Experimental lithotripter pulse at 16kV **(b)** Secondary acoustic emission detected using the NPL cavitation sensor

Physical Laboratory UK (NPL), **(14)** to record passive emissions from cavitation generated *in vitro* by an experimental lithotripter **(15)**. This paper reports on the analysis of these emissions and shows that they possess characteristics that depend on the degree of fragmentation of the stone.

Exploiting these preliminary results, some clinical prototypes (an example of which is displayed in *Figure 5*) were developed in collaboration with Precision Acoustics Ltd (PAL) UK. The prototypes have been patented **(16)** and they are currently being tested in the clinical environment.

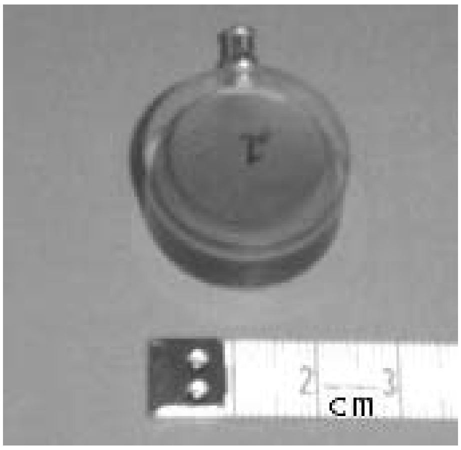


**Figure 5** Clinical prototype developed with PAL

## In vitro experiments

### *Experimental set-up*

*Figure 6* shows a diagram of the experimental set-up. Stone samples were placed at the focus of a bench top EM lithotripter in spherical holders (table-tennis balls) of 2cm diameter. Tests ensured that the holder walls did not significantly alter the lithotripter pressure field. A novel cylindrical broadband cavitation sensor **(14)**, made by NPL, was then coupled to the stone holder. The balls were each filled with different grades of sand, minimising the presence of entrained air bubbles: coarse sand (CS; grain diameter 10-30 mm); medium sand (MS; grain diameter 4-10 mm) or fine sand (FS; grain diameter 1-4mm).

These graded sand targets were used to simulate a stone at different well-characterised stages of fragmentation as it is encountered during the course of an ESWL treatment. One ball was filled with tap water (TW) to act as a control.

The discharge potential of the EM source was set and maintained at 16kV, which gave lithotripter shocks of 16MPa peak-positive pressure and 3MPa peak-negative pressure. The lithotripter pulses were measured using a Marconi Y-34-3598 PVDF bilaminar membrane hydrophone (sensitivity 53 mV/MPa). The detected signals were filtered using an analogue high pass filter with a cut-off frequency of 0.2MHz, to suppress most of the background noise due to the EM source itself. The filtered signals were acquired using a LeCroy 9354L digital scope with a sampling frequency of 100 Msamples/s and the digital data were transferred to a PC with a LabVIEW interface to be stored as text files. The stored data could then be processed using the MATLAB signal processing toolbox.

*Figure 7(a)* displays a 16 kV lithotripter pulse, measured as described above. The maximum positive pressure and the maximum negative pressure in the shock are respectively named peak-positive pressure and peak negative pressure. *Figure 7(b)* displays a typical output from the NPL cavitation sensor (currently uncalibrated). Two main bursts in the lower plot may be identified in the acoustic emission above the noise level. Previous work **(17)** indicates that these components are related respectively to the first and second collapse of microscopic bubbles (present in a cloud around the beam axis and in proximity of the stone **(18)**) during the shock-bubble interaction. The interval between these two bursts probably represents the mean interval ($t_c$) between the first and second rebound of each individual cavitation bubble during ESWL.

*continued on page 36*

# A new sensor for detecting and characterising acoustic cavitation in vivo during ESWL

*continued from page 35*

The interactions between a lithotripter pulse and a single bubble may be described adopting the Gilmore model of bubble dynamics **(13, 17)**. The fundamental assumptions of the model are: the bubble remains spherical throughout its motion; the radius of the bubble is much less than the wavelength of the applied field; the motion of the liquid is isentropic. The model has proved to be very useful even though only the second assumption is well satisfied in lithotripsy. *Figure 8* shows the results obtained for an ideal lithotripter pulse **(13, 17)** and a bubble of 6$\mu$m.

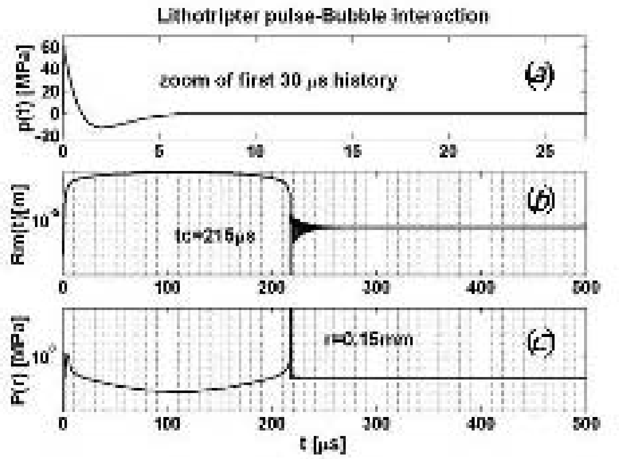


**Figure 8** Lithotripter pulse-bubble interaction according with the prediction of the Gilmore model of bubble dynamic The initial bubble radius was set to 6$\mu$m (a) Lithotripter pulse (b) Bubble radius (log-scale) (c) Pressure emitted by the bubble (log-scale)



When the lithotripter pulse passes over the location of the bubble, the bubble suddenly collapses (first collapse) emitting a pressure spike. It then rebounds and undergoes an explosive growth to collapse again (second collapse) after a time named collapse time ($t_c$), emitting another pressure pulse.

A parallel study to this project is attempting to simulate the emission emitted by a cloud of bubble during ESWL using a computational fluid dynamics code **(19)**.

## *Data analysis*

The collected data were analysed in both the time and frequency domain

## *Analysis in the time domain*

The signals were analysed off-line using MATLAB™. An adaptive threshold algorithm that automatically detects the two bursts in an emission signal has been developed.

It calculates their main parameters: duration, maximum amplitude and kurtosis *(Figure 9)*. In order to estimate $t_c$ the algorithm calculates the central times of the two bursts and estimates $t_c$ as the difference between these two times. This distinguishes the method of this paper from all previous studies **(17, 18)**, which estimated $t_c$ as the interval between the two maxima of the two bursts.

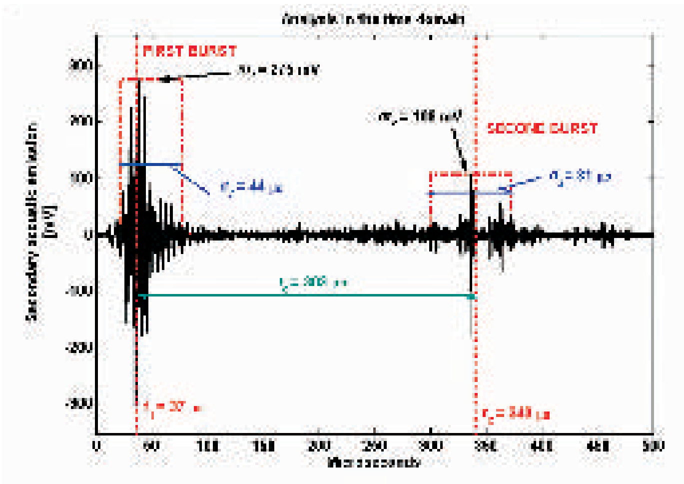


**Figure 9** Example of an analysis in the time domain, showing: the maximum amplitude of the first burst ($m_1$); the duration of the first burst ($d_1$); the central time of the first burst ($t_1$); the collapse time ($t_c$); the maximum amplitude of the second burst ($m_2$); the duration of the second burst ($d_2$); the central time of the second burst ($t_2$) The picture does not illustrate the kurtosis, which is a measure of how peaked are the bursts

## *Analysis in the frequency domain*

An algorithm analyses a set of traces recorded under the same conditions in order to extract the key frequency characteristics of the first and the second burst according to the following procedure.

Given the set of data, each burst is windowed and coherently averaged with the corresponding ones in the other recordings. Subsequently the Power Spectral Densities of the two averages obtained (one for the first burst and one for the second) and their central frequencies are estimated *(Figure 10)*.

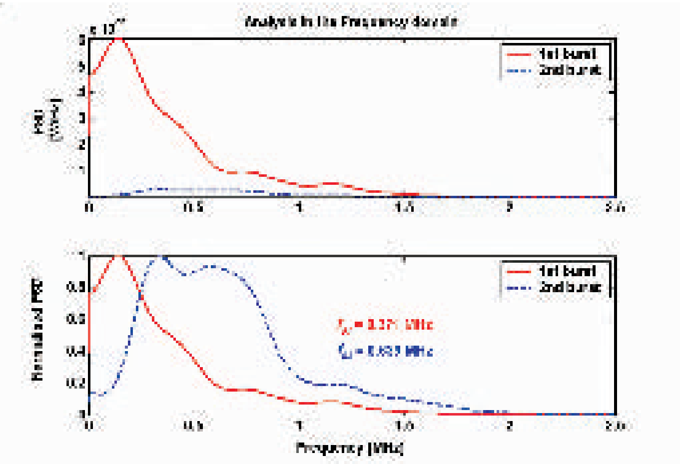


**Figure 10** Example of an analysis in the frequency domain PSDs of the two burst (upper box) Normalised PSDs (lower box)

## *Results: characterisation of cavitation in tap water*

The time domain analysis of the traces relative to the control sample, tap water, gave results in agreement with those of earlier experiments by the authors **(17, 18)**. The frequency domain analysis provided new information on the nature of the two bursts.

### *Time domain*

The data recorded with the NPL cavitation sensor showed a positive correlation between the collapse time $t_c$ (estimated as described above) and the peak negative pressure of the lithotripter pulse *(Figure 12)*. These results are in agreement with both the Gilmore model of bubble dynamics and previous experiments by the authors **(13, 17, 18)**. This tends to confirm the hypothesis that the NPL experimental sensor was recording essentially cavitation phenomena.

### *Frequency domain*

In each set of data the central frequency of the first burst is lower than that of the second burst. In particular the PSD of the first burst has its predominant component around 0.2MHz, which is the main frequency of the lithotripter pulse. The second burst that represents the activity of bubbles in free-evolution has a central frequency around 0.5MHz. Assuming that most of the bubble in the cloud has this resonant frequency, according to the Minnaert equation **(20)** ($f_0 \propto 1/R_0$) this gives a radius of 6$\mu$m (used in the Gilmore simulation).

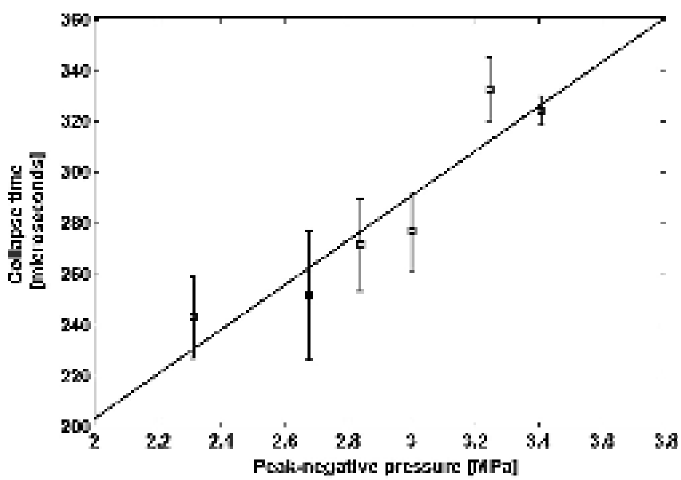


**Figure 11** Trend of the estimated collapse time $t_c$ with the peak-negative pressure. The error bars equal the ratio between the maximum error and the root square of the number of measurements per stone sample

## *Results: characterisation of cavitation adjacent to stone samples*

The results show a significant dependency of some of the cavitation emission parameters on the size of the stone fragments.

### *Time domain*

The collapse time $t_c$ *(Figure 12(a))* decreases significantly with the size of the fragments, implying that the size of the bubble present is related to that of the fragments **(20)**. The first burst contains both energy scattered from the incident lithotripter pulse; plus any cavitation emission. The amplitude *(Figure 12(b))* of the first burst clearly decreases with the size of the fragments, while its duration increases *(Figure 12(c))*. This may indicate less coherent scattering from the stone.

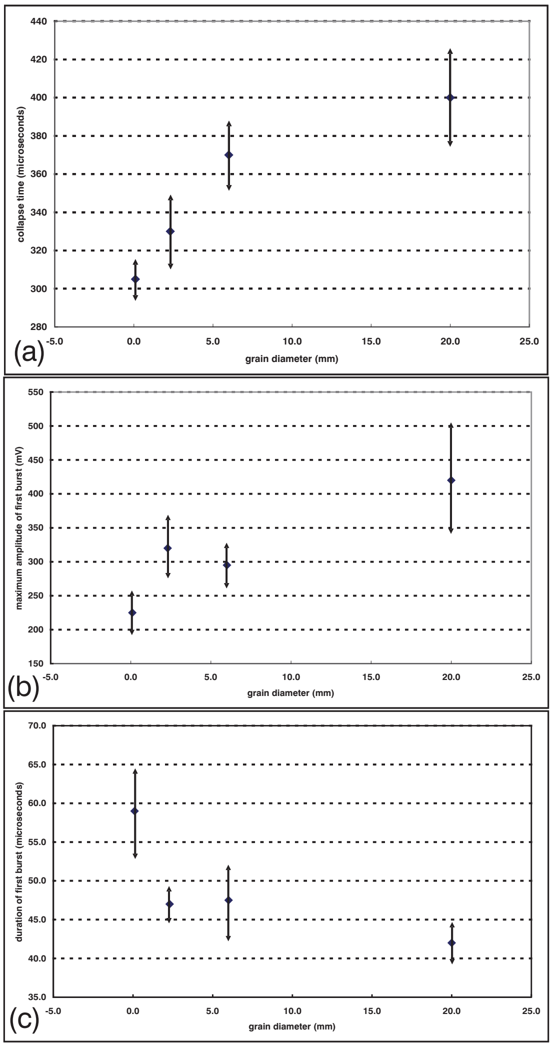


**Figure 12 (a)** collapse time $t_c$ **(b)** Maximum amplitude of the first burst **(c)** Duration of the first burst. The error bars equal the ratio between the maximum error and the root square of the number of measurements per stone sample. A grain diameter of zero indicates that the table-tennis ball was filled with tap water only

### *Frequency domain*

The central frequency *(Figure 13)* of the first burst is, for each sample, lower than that for the second burst

*continued on page 38*

# A new sensor for detecting and characterising acoustic cavitation in vivo during ESWL

*continued from page 37*

and close to the main frequency of the lithotripter pulse (0.2MHz). This result is in agreement with the hypothesis there is considerable scattering component of the first burst. Comparison of a set of measurements related to the same burst shows no significant difference between the frequencies of the different samples.

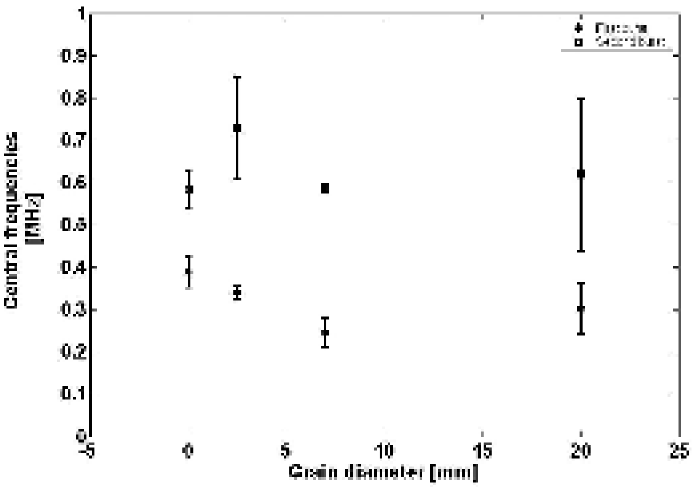


**Figure 13** Central frequencies of the two bursts. The error bars equal the ratio between the maximum error and the root square of the number of measurements per stone sample. A grain diameter of zero indicates that the table-tennis ball was filled with tap water only



## Design of a clinical prototype

The prototype *(Figure 5)* is a passive hydrophone made of a circular piezo-polymer PVdF element of 2cm diameter encapsulated in an external insulating shield. The size of the element has been designed to ensure that a path difference no greater than 0.1mm occurs for emissions coming from the kidney at 3MHz. The sensor is applied to the patient satisfying the restrictions of a class BF medical device according to the IEC60601-1.

## Test of the prototype in vitro

Several sets of recordings were made simultaneously using the NPL cavitation sensor and the PAL clinical prototype. The NPL was left at the focus of the lithotripter (coupled to the stone holder) while the PAL was placed at different positions laterally off-axis, facing the NPL and the stone. The PAL was placed off-axis to reproduce the configuration it would be *in vivo*, where it is not possible to place any sensor between the source and the stone, because this would interfere with the treatment itself. A correlation coefficient of 0.4 was found when the two sensors were close together (PAL 5mm off-axis), which decreased moving them further. *Figure 14* shows an example of the data recorded by the two sensors when they were close together.

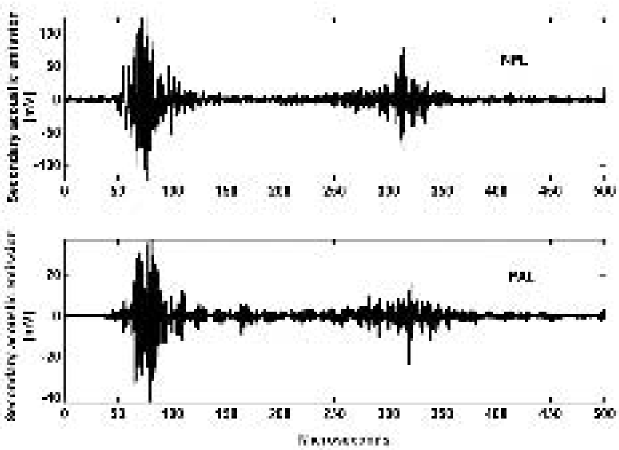


**Figure 14** Data simultaneously recorded by the NPL (upper box) and PAL (lower box) sensors

## Test of the prototype in vivo

The prototypes were tested on 40 consenting patients undergoing lithotripsy at Guy's and St Thomas' Hospital, after the design of the experiments was approved by the ethical committee of the hospital. The clinical lithotripter, at Guy's Hospital, London, is a Storz Modulith SLX-MX.

The sensor lead is connected to a portable digital oscilloscope (Tiepie Handyscope 3), which is in communication with a laptop (seen in foreground on the right of *figure 15*) through the USB port. The oscilloscope is automatically triggered by an electrical signal emitted by the EM source when it generates a shock. The digital scope does not require external power supply and the laptop is self-powered by its own battery (20V). Thus any possible connection between the patient and the main power supply is avoided and the sensor satisfies the restrictions of a class BF medical device according to the classification of the International Electrotechnical Commission (IEC60601-1). Prior to its use in the theatre, the equipment

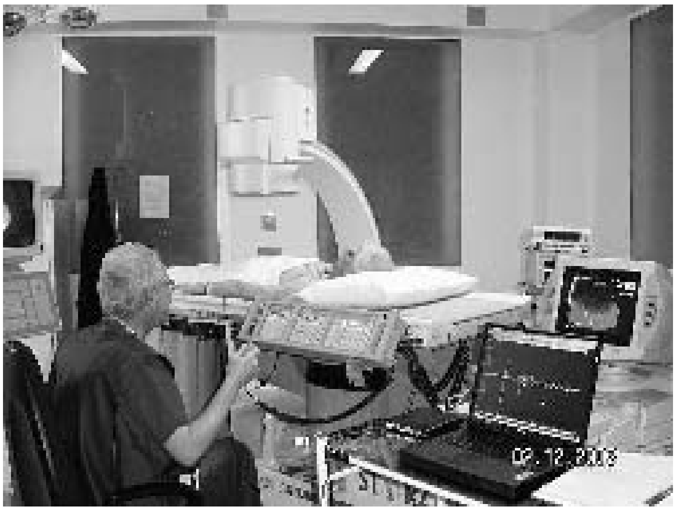

Figure 15 Experimental set-up in vivo

successfully passed electrical safety tests. The recorded traces are stored as text files using a software interface produced by Tiepie and subsequently analysed off-line.

*Figure 16* shows an example of secondary acoustic emissions recorded *in vivo*: at the beginning of a treatment section, using a calibrated PA prototype, a maximum emitted pressure of approximately 13kPa is recorded on the patient abdomen.

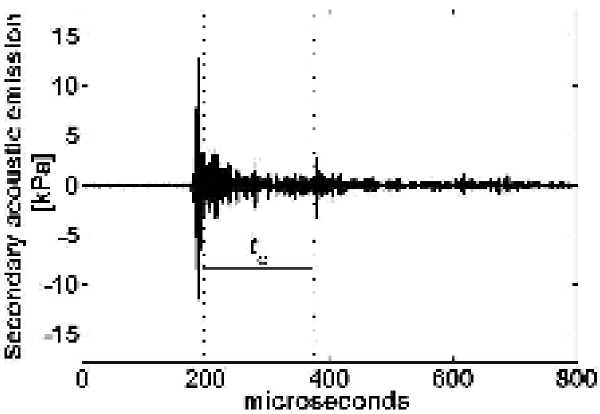


Figure 16 Secondary acoustic emissions recorded in vivo using a PAL calibrated prototype

## Conclusions

It has been shown *in vitro* that it is possible to use a passive acoustic device for diagnostic monitoring during lithotripsy, by exploiting the information carried by the passive cavitation emission. The prototype device has been tested in the clinic, and shown to be capable of detecting the first and second bursts of acoustic emission from the target. Preliminary analysis of the signal demonstrates similar features to those observed *in vitro*. Further work is needed to establish the parameters that correlate with the condition of the target material.

## Acknowledgments

This research was financed by the Engineering and Physical Sciences Research Council, UK GR/N19243. The authors thank Mrs Terri Gill at PAL, Dr Bajram Zeqiri and Ms Catherine Bickley at NPL, Mr Jonathan Glass, Mr Richard Tiptaff, Mr Simon Ryves and all the Lithotripsy Unit, the Mechanical Workshop and Electro Biomedical Engineering Section at Guy's and St Thomas' Hospital, London, for their collaboration.

## References

**1** C Chaussy, E Schmiedt, D Jocham, W Brendel, B Forssmann and V Walther, 'First clinical experience with extracorporeally induced destruction of kidney stones by shock waves 1981', *Journal of Urology* **167(5)** 1957-1960 (2002)

**2** H Iro, N Nitsche, J Meier, P M Wirtz and C H Ell, 'Piezoelectric shock wave lithotripsy of salivary gland stones: an in vitro feasibility study' *Journal of Lithotripsy Stone Disease* **3(3)** 211-216 (1991)

**3** M Maier, S Milz, T Tischer, W Munzing, N Manthey, A Stabler et al, 'Influence of extracorporeal shock-wave application on normal bone in an animal model in vivo Scintigraphy, MRI and histopathology' *J Bone Joint Surg Br* **84(4)** 592-599 (2002):

**4** C Von Eiff, J Overbeck, G Haupt, M Herrmann, S Winckler, KD Richter et al, 'Bactericidal effect of extracorporeal shock waves on Staphylococcus aureus' *J Med Microbiol:* **49(8)** 709-712 (2000)

**5** K T Ison, 'Physical and technical introduction to lithotripsy', in: MJ Coptcoat, RA Miller and JEA Wicklam Eds, 'Lithotripsy II Textbook of second generation extracorporeal lithotripsy', BDI Publishing, London, 7-12 (1987)

**6** D A Tolley and P Downey, 'Current advances in shock wave lithotripsy', *Current Opinion in Urology* **9(4)** 319-23 (1999)

**7** R M Schmitt, H Wuster, W Kraus and M Bibinger, 'The effects of errors in positioning lithotriptor and imaging kidney stones ultrasound', *Proc of Annual international conference of the IEEE Engineering in Medicine and Biology Society*, **Vol 12(1)**, 252-253 (1990)

**8** E Hausler, V Rech and M Wache M, 'Transient cavitation based ultrasonic lithotriptor positioning system', *Proc of the Annual international conference of the IEEE Engineering in Medicine and Biology Society*, **Vol 13**, 185-186 (1991)

**9** C C Chang, S M Liang, Y R Pu, C H Chen, I Manousakas, TS Chen et al, 'In vitro study of ultrasound based real-time tracking of renal stones for shock wave lithotripsy', *Journal of Urology*, **166(1)** 28-32 (2001)

**10** L Olsson, L O Almquist, A Grennberg and N G Holmer, 'Analysis and classification of secondary sounds from the disintegration of kidney stones with acoustic shock waves', *Ultrasound Med Biol*, **17(5)** 491-495 (1991)

**11** S Zhu, F H Cocks, G M Preminger and P Zhong, 'The role of stress waves and cavitation in stone comminution in shock wave lithotripsy', *Ultrasound in Medicine and Biology*, **28(5)** 661-671 (2002)

**12** W Sass, M Braunlich, H P Dreyer, E Matura, W Folberth, H G Preismeyer *et al* 'The mechanisms of stone disintegration by shock waves', *Ultrasound Med Biol*, **17(3)** 239-243 (1991)

**13** K B Cunningham, A J Coleman, T G Leighton and P R White, 'Characterising in vivo acoustic cavitation during lithotripsy with time-frequency methods', *Acoustics Bulletin*, **26(5)** 10-16 (2002)

**14** B Zeqiri, S C Davies, P N Gelat, M Hodnett and U I Lula, 'Novel sensors for monitoring acoustic cavitation', *Proc of IEEE Ultrasonics Symposium*, **Vol 1**, 417-420 (2000)

**15** F Fedele, A J Coleman and T G Leighton, 'Use of cylindrical PVdF hydrophone in a study of cavitation adjacent to stone phantoms during extracorporeal shockwave lithotripsy', *Proc of the IPEM Annual Scientific Meeting, 66* Bath, UK, September 2003

**16** T G Leighton, A J Coleman, F Fedele and P R White, 'A passive acoustic system for evaluating the in vivo performance of extracorporeal shock wave lithotripsy', UK Patent Application No 03198637 (2003)

**17** A J Coleman, M J Choi, J E Saunders, T G Leighton, 'Acoustic emission and sonoluminescence due to cavitation at the beam focus of an electrohydraulic shock wave lithotripter', *Ultrasound in Medicine and Biology*, **18** 267-281 (1992)

**18** A J Coleman, M Whitlock, T Leighton and J E Saunders, 'The spatial distribution of cavitation induced acoustic emission, sonoluminescence and cell lysis in the field of a shock wave lithotripter', *Phys Med Biol*, **38(11)** 1545-1560 (1993)

**19** A R Jamaluddin, G J Ball and T G Leighton, 'Free-Lagrange simulations of shock/bubble interaction in shock wave lithotripsy' *Proceedings of the Second International Conference on Computational Fluid Dynamics*, 541-5461 (2002)

**20** T G Leighton, 'The Acoustic Bubble', Academic Press, London (1994)

**F Fedele**, *Medical Physics Department, Guy's and St. Thomas' NHS Trust, UK and the Institute of Sound and Vibration Research, University of Southampton, UK;* **A J Coleman,** *Medical Physics Department, Guy's and St. Thomas' NHS Trust;* **T G Leighton** *and* **P R White**, *Institute of Sound and Vibration Research, University of Southampton; and* **A M Hurrell,** *Precision Acoustics Ltd., UK*